



HHS Public Access

Author manuscript

ACS Catal. Author manuscript; available in PMC 2023 October 19.

Published in final edited form as:

ACS Catal. 2022 August 05; 12(15): 9801–9805. doi:10.1021/acscatal.2c02294.

Radical Termination via β -Scission Enables Photoenzymatic Allylic Alkylation Using “Ene”-Reductases

Netgie Laguerre[‡],

Paul S. Riehl[‡],

Daniel G. Oblinsky,

Megan A. Emmanuel,

Michael J. Black,

Gregory D. Scholes,

Todd K. Hyster^{*}

Department of Chemistry, Princeton University, Princeton, New Jersey 08544, United States

Department of Chemistry and Chemical Biology, Cornell University, Ithaca, New York 14850, United States

Abstract

Allylations are practical transformations that forge C–C bonds while introducing an alkene for further chemical manipulations. Here, we report a photoenzymatic allylation of α -chloroamides with allyl silanes using flavin-dependent ‘ene’-reductases (EREDs). An engineered ERED can catalyze annulative allylic alkylation to prepare 5, 6, and 7-membered lactams with high levels of enantioselectivity. Ultrafast transient absorption spectroscopy indicates that radical termination occurs via β -scission of the silyl group to afford a silyl radical, a distinct mechanism by comparison to traditional radical allylations involving allyl silanes. Moreover, this represents an alternative strategy for radical termination using EREDs. This mechanism was applied to intermolecular couplings involving allyl sulfones and silyl enol ethers. Overall, this method highlights the opportunity for EREDs to catalyze radical termination strategies beyond hydrogen atom transfer.

Graphical Abstract

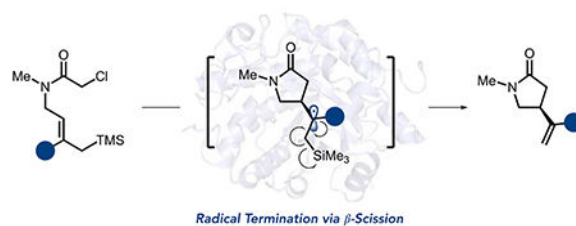
^{*}Corresponding Author: thyster@cornell.edu.

[‡]These authors contributed equally.

The Supporting Information is available free of charge at <https://pubs.acs.org/>

Supplemental figures, detailed experimental procedures, spectroscopy information, characterization data (NMR spectra and HPLC traces) (PDF)

The authors declare no competing financial interest.



Keywords

biocatalysis; flavin; radical; allylation; photochemistry

Asymmetric Csp³–Csp³ bond formation is indispensable for constructing societally essential molecules.¹ Consequently, numerous catalytic methods have been developed to facilitate their construction.² Among these, reactions involving open-shell radical intermediates are desirable because they have low activation barriers and can form sterically congested centers.³ However, strategies for rendering these transformations asymmetric remain underdeveloped compared to reactions involving other types of reactive intermediates.⁴

Enzymes are ideal catalysts for asymmetric synthesis because they can precisely orient reactive intermediates, and their activity can be optimized using directed evolution.⁵ However, biocatalysts are often restricted to their natural reaction mechanisms, limiting their ability to address selectivity challenges in chemical synthesis.⁶ An ongoing goal in the field has been to develop strategies to expand the synthetic capabilities of enzymes.⁷ We recently demonstrated that flavin-dependent ‘ene’-reductases (EREDs) could catalyze non-natural C–C bond-forming reactions involving radical intermediates.⁸ In nature, EREDs catalyze the reduction of activated alkenes via a hydride transfer mechanism.⁹ We found that these enzymes will template charge-transfer (CT) complexes between various alkyl halides and the reduced flavin hydroquinone (FMN_{hq}) cofactor. Irradiation with visible light promotes an electron from the cofactor to the substrate. Upon mesolytic cleavage of the carbon–halogen bond, an alkyl radical is formed that can react with an alkene to forge a new C–C bond with high selectivity. Thus far, our studies have focused on radical termination via hydrogen atom transfer (HAT) from flavin semiquinone (FMN_{sq}) (Figure 1a).¹⁰ To expand the synthetic utility of these catalysts, we sought to develop alternative radical termination mechanisms.

Radical allylations are attractive reactions because they form a new C–C bond while also introducing a handle for subsequent functionalizations.¹¹ The most common reagents for these reactions are allyl stannanes, silanes, and sulfones. In these reactions, the reagent largely dictates the mechanism of elimination. For allyl stannanes and sulfones, radical termination occurs via β -scission to produce stannyl or sulfinyl radicals (Figure 1b).¹² As C–Si (76 kcal/mol) bonds are stronger than C–Sn (45 kcal/mol) or C–SO₂Ar (65 kcal/mol), allyl silanes typically undergo different elimination mechanisms.¹³ In atom transfer reactions, the alkyl radical is trapped by a halide, followed by thermal elimination to form an alkene and halosilane (Figure 1b).¹⁴ Alternatively, the presence of an oxidant can enable a radical-polar crossover mechanism where the radical is oxidized to the β -silyl cation,

which readily eliminates (Figure 1b).¹⁵ We hypothesized that a β -scission or polar crossover mechanism would be available to EREDs. However, it was unclear whether either of these mechanisms could be competitive with HAT (Figure 1c).

We tested the viability of the proposed reactivity in the cyclization of allyl silane **1** to afford γ -lactam **2**. We found that GluER-T36A with an NADPH turnover system consisting of glucose as a terminal hydride source and glucose dehydrogenase (GDH) under visible light irradiation, afforded the desired product in 64% yield and >99:1 er, with < 5% yield of the reductive cyclization product **3** (Table 1, entry 1). A brief screening of GluER variants previously engineered in-house revealed that GluER-T36A-K317M-Y343F (GluER-G6) was the optimal enzyme (Table 1, entry 2).¹⁶ A control experiment confirmed that the cofactor turnover system is required to achieve high yields (Table 1, entry 3). Continuous light irradiation of GluER-G6 in buffer, without any turnover system present, is sufficient to generate both FMN_{hq} and FMN_{sq} in the protein active site (Supplemental Figure 9).¹⁷ The addition of cofactor turnover system favors formation of FMN_{hq}, the oxidation state responsible for radical initiation. A control experiment confirms that radical initiation cannot occur from ground state FMN_{hq} (Table 1, entry 4).¹⁸ Additionally, when GluER-G6 is photoreduced for 72 hours to generate a mixture of the FMN_{sq} and FMN_{hq} and then substrate is added after photoirradiation was stopped, no product is formed (Table 1, entry 5). These results indicate that radical initiation does not occur from either the ground state FMN_{sq} or FMN_{hq}. While initial screens were run with six equivalents of glucose, we found that two equivalents provided comparable yields (Table 1, entry 6). Finally, we ran the reaction on a preparative scale using 0.75 mol % of GluER-G6 and isolated the desired lactam product in 46% yield with >99:1 er (Table 1, entry 7).

With the optimized conditions in hand, we explored the scope of the transformation (Figure 2). GluER-G6 accommodates substituents at the *ortho*-, *meta*-, and *para*-positions of the aromatic ring (Figure 2, **4–7**). Electron-rich substrates are more reactive than electron-deficient ones. However, the enantioselectivity is high in all cases. Unsubstituted alkenes are also effective for both 5-*exo-trig* and 6-*exo-trig* cyclization, affording products in high yields but with modest levels of enantioselectivity (Figure 2, **8, 9, 10**). We attribute the low enantioselectivity to the lack of substituents on the alkene moiety to help orient the substrate within the protein active site. This enzyme can also catalyze 7-*exo-trig* cyclizations in promising yields and enantioselectivities. Beyond aromatic substituents, aliphatic substituents are also tolerated. While the methyl-substituted substrates are only modestly selective (Figure 2, **12**), larger *i*-propyl and *c*-hexyl substituents provide synthetically useful levels of enantioselectivity (Figure 2, **13**, and **14**). Furthermore, we found that heterocycles, such as furan, were also well tolerated (Figure 2, **15**).

While evaluating the substrate scope, we found that aromatic substrates containing electron-withdrawing substituents provided lower yields of the desired product compared to those with electron-donating substituents. For example, *meta*-CF₃ amide **16** afforded the allylated product **17** in only 3% yield. Upon further analysis, we found that the reductively cyclized product **18** is formed in 34% yield (Figure 3a). While performing a direct Hammett analysis might be difficult because substitution impacts substrate binding, this result suggests that

more electrophilic radicals favor radical termination via hydrogen atom transfer rather than elimination.¹⁹

Next, we sought to interrogate the mechanism of radical termination. We envisioned two possibilities, i) a radical-polar crossover mechanism where the β -silyl radical is oxidized by FMN_{sq}, forming FMN_{hq} and a β -silyl cation that can eliminate to form the alkene and silanol, or ii) β -scission of the β -silyl radical producing the product and a silyl radical which can abstract a hydrogen atom from FMN_{sq} to produce oxidized FMN. As the final flavin oxidation state differs between these two mechanisms, they can be distinguished using transient absorption spectroscopy.

Transient absorption spectroscopy (TAS) studies were conducted in a sealed quartz cuvette containing GluER-G6 reduced with sodium dithionite and chloroamide **1**. The sample was excited with a 370 nm pulse and UV-Vis probe spectrum (400 – 750nm) was taken over various pump-probe delay times (maximum delay of 1000 ns). As these spectra contain multiple species, deconvolution was performed using global analysis and compared to the results of data obtained in our previous ERED catalyzed reductive cyclizations.¹⁰ The first-time component is mesolytic cleavage occurring with a lifetime of 10 ps, mirroring what was observed in the reductive cyclizations. This is followed by the growth a broad spectral feature that decays with a lifetime of 38 ns. As we know cyclization is fast (<700 ps) for structurally similar substrates used for reductive cyclizations, we attribute this feature to the TMS radical group undergoing β -scission.¹⁶ The extended lifetime of the radical intermediate is potentially due to stabilization of the radical by the electropositive β -silyl group.²⁰ The spectrum formed after β -scission is consistent with the absorption profile of the neutral flavin semiquinone. This feature persists with a lifetime of 150 ns before decaying to the flavin quinone. This suggests that the silyl radical formed after β -scission abstracts a hydrogen atom from the neutral flavin semiquinone to form silane and flavin quinone (Figure 3b). In traditional radical chemistry, this mechanism is disfavored because of the strength of the C–Si bond. It is possible that this mechanism is available under biocatalytic conditions through the intermediacy of a silicon-ate complex.

Our previous studies indicate that this initiation event occurs via photoexcitation of an enzyme templated charge transfer complex that forms between the substrate and FMN_{hq}. To confirm that this mechanism remains the case for these substrates, we prepared a sample with reduced GluER-G6 (containing FMN_{hq}) and added the substrate. Consistent with our previous studies, we observed a new absorption band at 495 nm, suggesting the intermediacy of a CT complex (Figure 3c).

Having established that EREDs can catalyze intramolecular allylations, we explored whether they could facilitate intermolecular reactions. Using GluER-G6 under the standard reaction conditions, we found that chloroacetamide **19** could be coupled to trimethylallylsilane **20** to afford the γ,δ -unsaturated amide **23** in 61% yield (Figure 4). Beyond allyl silanes, silyl enol ether **22** is reactive and affords a 1,4-dicarbonyl product **24** in nearly quantitative yield. Finally, we hypothesized that allyl sulfones could be effective reagents for radical allylation because of their propensity to undergo β -scission elimination. When amide **19** is supplied

with allylsulfone **21**, the allylated product **23** is formed in 73% yield.²¹ Collectively, these examples suggest the generality of this radical termination mechanism.

In conclusion, we have demonstrated that EREDs can catalyze asymmetric allylations using allyl silanes and allyl sulfones. Radical termination occurs via a β -scission mechanism that is competitive with hydrogen atom transfer from FMN_{sq}. Beyond offering a new mechanism, this substitution pattern significantly expands the lifetime of radical intermediates within the protein active site. These observations offer new insights into non-natural chemistry with EREDs and unlock synthetic opportunities of this enzyme-catalyzed platform to enable novel, selective radical-based transformations as solutions to unaddressed selectivity challenges in radical chemistry.

Supplementary Material

Refer to Web version on PubMed Central for supplementary material.

ACKNOWLEDGMENT

Financial support for reaction development and evaluation of the scope was provided by the NIH (R01 GM127703). Mechanistic studies were supported by the Division of Chemical Science, Geosciences, and Biosciences, Office of Basic Energy Sciences of the U.S. Department of Energy through Grant DE-SC0019370. NL was supported by an NSF-GFRP. DGO was supported by the Postgraduate Scholarships Doctoral Program of NSERC. This work made use of the Cornell University NMR Facility, which is supported, in part, by the NSF through MRI Award CHE-1531632. The authors thank Ivan Keresztes for assistance in analyzing and collecting spectra.

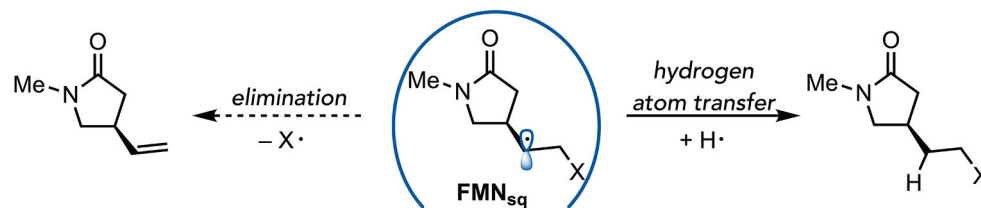
REFERENCES

1. (a)Williams K; Lee E Importance of Drug Enantiomers in Clinical Pharmacology. *Drugs* 1985, 30, 333–354. [PubMed: 3905334] (b)Lovering F, Bikker J & Humblet C Escape from Flatland: Increasing Saturation as an Approach to Improving Clinical Success. *J. Med. Chem* 2009, 52, 6752–6756. [PubMed: 19827778]
2. (a)Bar G; Parsons AF Stereoselective radical reactions. *Chem. Soc. Rev* 2003, 32, 251–263. [PubMed: 14518178] (b)Choi J; Fu GC Transition metal-catalyzed alkyl-alkyl bond formation: another dimension in cross-coupling chemistry. *Science* 2017, 356, eaaf7230.(c)Chen Z; Rong M, Nie J, Zhu X, Shi B Ma J Catalytic alkylation of unactivated C(sp³)-H bonds for C(sp³)-C(sp³) bond formation. *Chem. Soc. Rev* 2019, 48, 4921–4942. [PubMed: 31403147] (d)Trost BM, Vranken DL Asymmetric Transition Metal-Catalyzed Allylic Alkylations. *Chem Rev* 1996, 96, 395–422. [PubMed: 11848758] (e)Meggers E Asymmetric catalysis activated by visible light. *Chem. Commun* 2015, 51, 3290–3301.
3. (a)Studer A; Curran DP Catalysis of Radical Reactions: A Radical Chemistry Perspective. *Angew. Chem. Int. Ed* 2016, 55, 58–102.(b)Prier CK; Ranik DA; MacMillan DWC Visible Light Photoredox Catalysis with Transition Metal Complexes: Applications in Organic Synthesis. *Chem. Rev* 2013, 113, 5322–5363. [PubMed: 23509883] (c)Romero NA; Nicewicz DA Organic Photoredox Catalysis. *Chem. Rev* 2016, 116, 10075–10166. [PubMed: 27285582] (d)Skubi KL; Blum TR; Yoon TP Dual catalysis strategies in photochemical synthesis. *Chem. Rev* 2016, 116, 10035–10074. [PubMed: 27109441] (e)Twilton J; Le C; Zhang P; Shaw MH; Evans RW; MacMillan DWC The merger of transition metal and photocatalysis. *Nat. Chem. Rev* 2017, 1, 0052.
4. (a)Sibi MP; Manyem S; Zimmerman J Enantioselective Radical Processes. *Chem. Rev* 2003, 103, 3263–3295. [PubMed: 12914498] (b)Miyabe H; Kawashima A; Yoshioka, Eito; Kohtani, S. Progress in Enantioselective Radical Cyclizations. *Chem. Eur. J* 2017, 23, 6225–6236. [PubMed: 28120354] (c)Nicewicz DA; MacMillan DWC Merging Photoredox Catalysis with Organocatalysis: the Direct Asymmetric Alkylation of Aldehydes. *Science* 2008, 322, 77–80. [PubMed: 18772399] (d)Du J; Skubi KL; Schultz DM; Yoon T A Dual-Catalysis Approach to Enantioselective [2 + 2] Photocycloadditions Using Visible Light. *Science* 2014, 344, 392–396. [PubMed: 24763585]

- (e)Huo H; Shen X; Wang C; Zhang L; Rose P; Chen L; Harms K; Marsch M; Hilt G; Meggers E Asymmetric photoredox transition-metal catalysis activated by visible light. *Nature* 2014, 515, 100–103. [PubMed: 25373679] (f)Rono LJ; Yayla HG; Wang DY; Armstrong MF; Knowles RR Enantioselective Photoredox Catalysis Enabled by Proton-Coupled Electron Transfer: Development of an Asymmetric Aza-Pinacol Cyclization. *J. Am. Chem. Soc* 2013, 135, 17735–17738. [PubMed: 24215561] (g)Blum TR; Miller ZD; Bates DM; Guzei IA; Yoon TP Enantioselective photochemistry through Lewis acid-catalyzed triplet energy transfer. *Science* 2016, 354, 1391–1395. [PubMed: 27980203]
5. (a)Yi Dong; Bayer T; Badenhorst CPS; Wu S; Doerr M; Hohne M; Bornscheuer UT Recent trends in biocatalysis *Chem. Soc. Rev* 2021, 50, 8003–8049. [PubMed: 34142684] (b)Devine PN, Howard RM, Kumar R; Thompson MP; Truppo MD; Turner NJ Extending the application of biocatalysis to meet the challenges of drug development. *Nat. Rev. Chem* 2018, 2, 409–421. (c)Savile CK; Janey JM; Mundorff EC; Moore JC; Tam S; Jarvis WR; Colbeck JC; Krebber A; Fleitz FJ; Brands J; Devine PN; Huisman GW; Hughes GJ Biocatalytic Asymmetric Synthesis of Chiral Amines from Ketones Applied to Sitagliptin Manufacture. *Science* 2010, 329, 305–309. [PubMed: 20558668] (d)Hall M Enzymatic strategies for asymmetric synthesis. *RSC Chem. Biol* 2021, 2, 958–989.
6. (a)Sheldon RA; Brady D; Bode ML The Hitchhiker’s guide to biocatalysis: recent advances in the use of enzymes in organic synthesis. *Chem. Sci* 2020, 11, 2587–2605. [PubMed: 32206264] (b)Schmidt NG; Eger E; Kroutil W Building Bridges: Biocatalytic C–C-Bond Formation toward Multifunctional Products. *ACS Catal* 2016, 6, 4286–4311. [PubMed: 27398261]
7. (a)Hammer SC; Knight AM; Arnold FH Design and evolution of enzymes for non-natural chemistry. *Curr. Opin. Green Sustain. Chem* 2017, 7, 23–30. (b)Schwizer F; Okamoto Y; Heinisch T; Gu Y; Pellizzoni MM; Lebrun V; Reuter R; Köhler V; Lewis JC; Ward TR Artificial Metalloenzymes: Reaction Scope and Optimization Strategies. *Chem Rev* 2018, 118, 142–231. [PubMed: 28714313] (c)Bornscheuer UT The fourth wave of biocatalysis is approaching. *Phil. Trans. T. Soc. A* 2017, 376.20170063.
8. (a)Black MJ; Biegasiewicz KF; Meichan AJ; Oblinsky DG; Kudisch B; Scholes GD; Hyster TK Asymmetric redox-neutral radical cyclization catalysed by flavin-dependent ‘ene’-reductases. *Nat. Chem* 2020, 12, 71–75. [PubMed: 31792387] (b)Clayman PD; Hyster TK Photoenzymatic Generation of Unstabilized Alkyl Radicals: An Asymmetric Reductive Cyclization. *J. Am. Chem. Soc* 2020, 142, 15673–15677. [PubMed: 32857506] (c)Gao X; Turek-Herman JR; Choi YJ, Cohen RD; Hyster TK Photoenzymatic Synthesis of α -Tertiary Amines by Engineered Flavin-Dependent “Ene”-Reductases. *J. Am. Chem. Soc* 2021, 143, 19643–19647. [PubMed: 34784482]
9. Roy TK; Sreedharan R; Ghosh P; Gandhi T; Maiti D Ene-Reductase: A Multifaceted Biocatalyst in Organic Synthesis *Chem. Eur. J* 2022 e202103949.
10. (a)Biegasiewicz KF; Cooper SJ; Gao X; Oblinsky DG; Kim JH; Garfinkle SE; Joyce LA; Sandoval BA; Scholes GD; Hyster TK Photoexcitation of flavoenzymes enables a stereoselective radical cyclization *Science* 2019, 364, 1166–1169. [PubMed: 31221855] (b)Page C; Cooper SJ; DeHovitz JS; Oblinsky DG; Biegasiewicz KF; Antropow AH; Armbrust KW; Ellis JM; Hamann LG; Horn EJ; Oberg KM; Scholes G; Hyster TK Quaternary Charge-Transfer Complex Enables Photoenzymatic Intermolecular Hydroalkylation of Olefins. *J. Am. Chem. Soc* 2021, 143, 97–102. [PubMed: 33369395] (c)Huang X; Wang B; Wang Y; Jiang G; Feng J; Zhao H Photoenzymatic enantioselective intermolecular radical hydroalkylation. *Nature* 2020, 584, 69–74. [PubMed: 32512577]
11. (a)Huang M; Bellotti P; Glorius F Transition metal-catalysed allylic functionalization reactions involving radicals. *Chem. Soc. Rev* 2020, 49, 6186–6197. [PubMed: 32756671] (b)Tucker JW; Nguyen JD; Narayanam JMR; Krabbe SW; Stephenson CRJ Tin-free radical cyclization reactions initiated by visible light photoredox catalysis. *Chem. Commun* 2010, 46, 4985. (c)Mastracchio A; Warkentin AA; Walji AM; MacMillan DWC Direct and enantioselective α -allylation of ketones via singly occupied molecular orbital (SOMO) catalysis. *Proc. Natl. Acad. Sci. U.S.A* 2010, 107, 20648–20651. [PubMed: 20921367] (d)Pham PV; Ashton K; MacMillan DWC The intramolecular asymmetric allylation of aldehydes via organo-SOMO catalysis: A novel approach to ring construction. *Chem. Sci* 2011, 2, 1470–1473. [PubMed: 23087809] (e)Mizuta S; Engle KM; Verhoog S; Galicia-López O; O’Duill M; Médebielle, Wheelhouse K; Rassias G; Thompson AL; Gouverneur V Trifluoromethylation of Allylsilanes under Photoredox Catalysis. *Org. Lett* 2013, 15, 1250–1253. [PubMed: 23465076]

12. (a)Quiclet-Sire B; Zard SZ New Radical Allylation Reaction. *J. Am. Chem. Soc* 1996, 118, 1209–1210.(b)Sibi MP; Ji J Acyclic Stereocontrol in Radical Reactions. Diastereoselective Radical Addition/Allylation of N-Propenyloxazolidinone. *J. Org. Chem* 1996, 61, 6090–6091. [PubMed: 11667436] (c)Curran DP; Chen MH; Spletzer E; Seong CM; Chang CT Atom transfer cyclization reactions of hex-5-ynyl iodides: synthetic and mechanistic studies. *J. Am. Chem. Soc* 1989, 111, 8872–8878.(d)Structural and Chemical Properties of Silyl Radicals. Chatgililoglu, C. *Chem. Rev* 1995, 95, 1229.
13. Luo Y-R; Cheng J-P in *CRC Handbook of Chemistry & Physics 94th Edn* (ed. Haynes WM) 9–65 (CRC, 2013).
14. Porter NA; Wu JH; Zhang G; Reed AD Enantioselective Free Radical Allyl Transfers from Allylsilanes Promoted by Chiral Lewis Acids. *J. Org. Chem* 1997, 62, 6702–6703.
15. (a)Pitzer L; Schwarz JL; Glorius F Reductive radical-polar crossover: traditional electrophiles in modern radical reactions. *Chem Sci* 2019, 10, 8285–8291. [PubMed: 32055300] (b)Sharma S; Singh J; Sharma A Visible Light Assisted Radical-Polar/Polar-Radical Crossover Reactions in Organic Synthesis. *Adv. Synth. Catal* 2021,363, 3146–3169.
16. Nicholls BT; Oblinsky DG; Kurtoic SI; Grosheva D; Ye Y; Scholes GD; Hyster TK Engineering a Non-Natural Photoenzyme for Improved Photon Efficiency. *Angew. Chem. Int. Ed* 2022, 61 e202113842.
17. Massey V; Stankovich M; Hemmerich P Light-Mediated Reduction of Flavoproteins with Flavins as Catalysts. *Biochemistry* 1978, 17, 1–8. [PubMed: 618535]
18. Fu H; Lam H; Emmanuel MA; Kim J; Sandoval B; Hyster TK Ground-State Electron Transfer as an Initiation Mechanism for Biocatalytic C–C Bond Forming Reactions. *J. Am. Chem. Soc* 2021, 143, 9622–9629. [PubMed: 34114803]
19. (a)Vleschouwer FD; Speybroeck VV; Waroquier M; Geerlings P; Proft FD Electrophilicity and Nucleophilicity Index for Radicals. *Org Lett* 2007, 9, 14, 2721–2724.(b)Fisher H; Radom L Factors Controlling the Addition of Carbon-Centered Radicals to Alkenes—An Experimental and Theoretical Perspective. *Angew. Chem. Int. Ed* 2001, 40, 1340–1371.(c)Héberger K; Lopata AJ Assessment of Nucleophilicity and Electrophilicity of Radicals, and of Polar and Enthalpy Effects on Radical Addition Reactions. *Org. Chem* 1998, 63, 8646–8653.
20. Parasee F; Senarathna MC; Kannangara PB; Alexander SN; Arche PDE; Weilin E Radical philicity and its role in selective organic transformations. *Nat. Chem. Rev* 2021, 5, 486–499.
21. Replacing the TMS group with phenylsulfone for unsubstituted 5 exo substrate 8S-B affords product in 25% yield with 78:22 er.

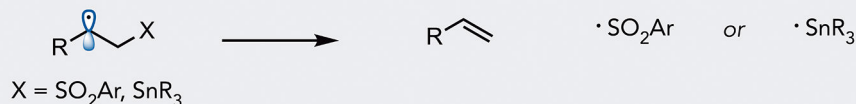
A. Radical Termination in Photoenzymatic Reactions



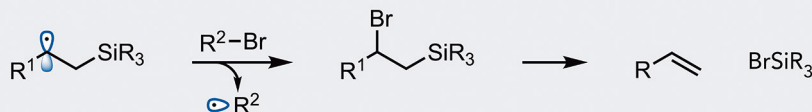
Can EREDs Use Elimination Mechanisms for Radical Termination?

B. Elimination Mechanisms Involving Radical Intermediates

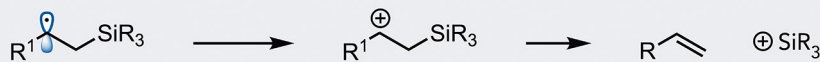
- ***β-Scission***



- ***Atom Transfer***



- ***Polar Crossover***



C. Proposed - Photoenzymatic Radical Allylation

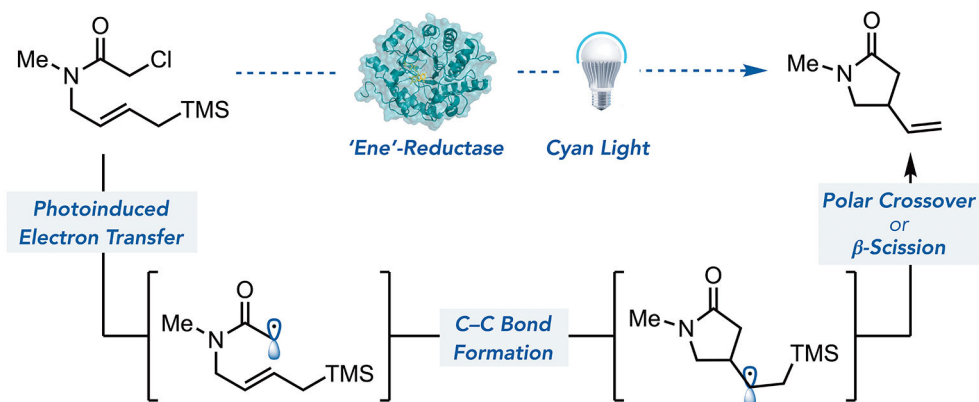
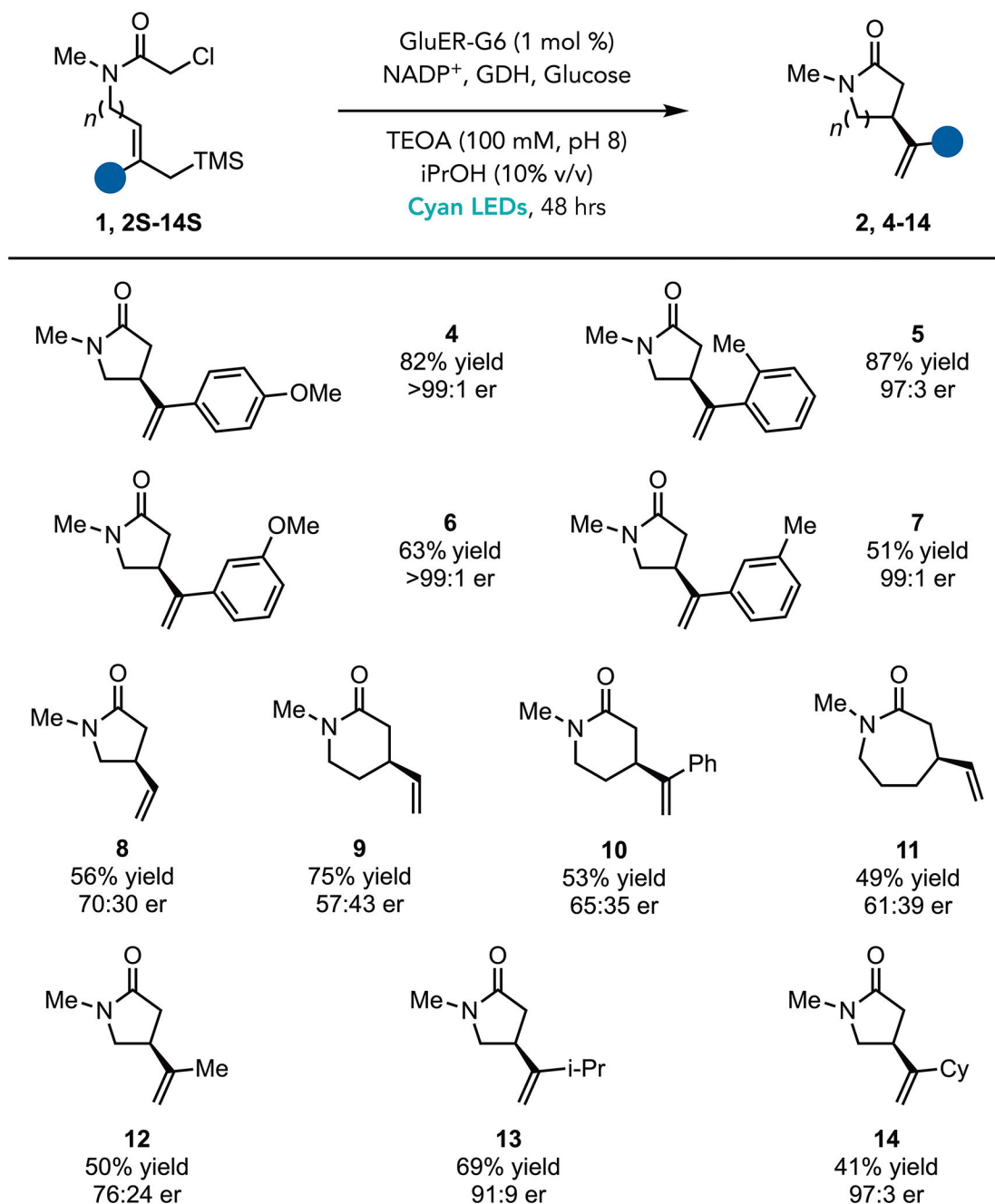


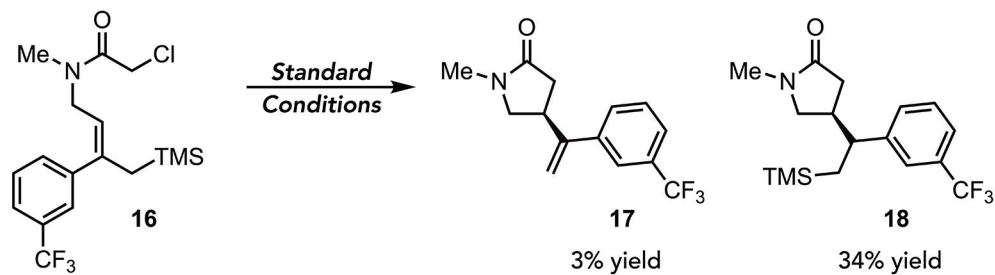
Figure 1.
Mechanisms of Radical Allylation

**Figure 2.**

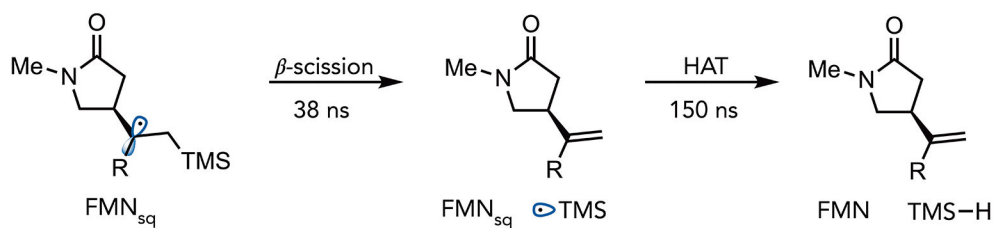
Substrate Scope

a. Reaction conditions: amide (20 μmol), purified GluER enzyme (1 mol%, 200 nmol), 100 mM buffer (18 mM final substrate concentration), iPrOH (10 % v/v), glucose (40 μmol), GDH-105 (10 wt%, 0.4–7.5 mg/rxn), NADP⁺ (2 mol%), 48 hours, 25 °C. Yields were determined by NMR analysis using trimethoxy benzene as an internal standard. See Supplemental Information for detailed experimental procedure and additional optimization studies.

A. Competitive Reductive Cyclization



B. Radical Termination Mechanism



C. UV-Vis Absorption for the Enzyme-Templated CT Complex

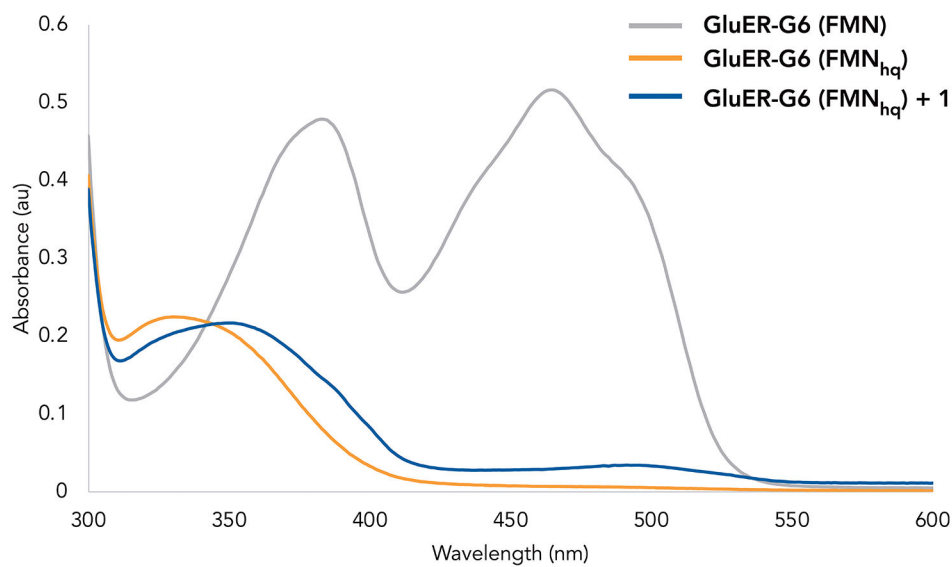
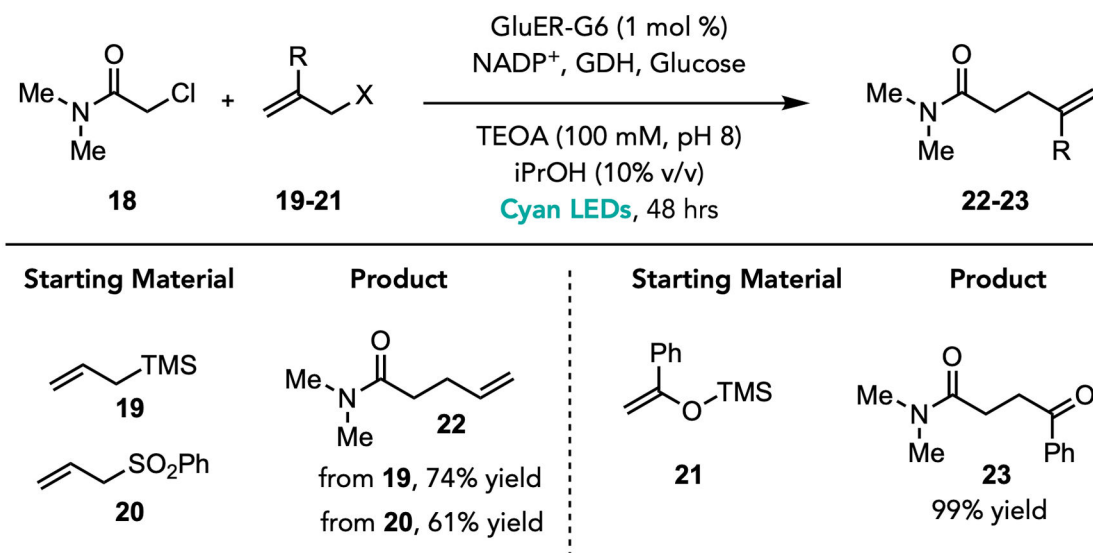


Figure 3.
Electronic Effects on Reaction Outcome

**Figure 4.**

Intermolecular Allylation

a. Reaction conditions: **18** (20 μmol , 2.06 μL), **19–21** (80 μmol) purified GluER enzyme (1 mol%, 200 nmol), 100 mM buffer (18 mM final substrate concentration), iPrOH (10 % v/v), glucose (40 μmol), GDH-105 (10 wt%, 0.4–7.5 mg/txn), NADP⁺ (2 mol%), 48 hours, 25 °C. Yields were determined by HPLC using calibration curves. See Supplemental Information for detailed experimental procedure and additional optimization studies.

Table 1.

Reaction Optimization

Entry	Deviation from "Initial Conditions"	Yield (%)	e.r.
1	none	64	99:1
2	GluER-G6 instead of GluER-T36A	92	99:1
3	GluER-G6 and no cofactor turnover system	72	99:1
4	GluER-G6 and no light	0	n.d.
5	GluER-G6 without cofactor turnover system and photoreduction of the enzyme prior to addition of the substrate	0	n.d.
6	GluER-G6 and 2 equiv. of Glucose	92	99:1
7	0.24 mmol scale at 43.6 mM using KRED P103	46	99:1

^aReaction conditions: **1** (10 μ mol, 3.1 mg), purified GluER enzyme (1 mol%, 100 nmol), 100 mM buffer (18 mM final substrate concentration), iPrOH (10 % v/v), glucose (60 μ mol), GDH-105 (10 wt%, 0.3 mg/rxn), NADP⁺ (2 mol%), 24 hours, 25 °C. Yields determined by HPLC using a calibration curve for Entries 1–6. Reported yield for Entry 7 was for isolated and purified material. See Supplemental Information for detailed experimental procedure and additional optimization studies.